Title

Spinal activity of interleukin 6 mediates myelin basic protein-induced allodynia

Authors

Ko, Justin S
Eddinger, Kelly A
Angert, Mila
et al.

Publication Date

2016-08-01

DOI

10.1016/j.bbi.2016.03.003

Peer reviewed

HHS Public Access

Author manuscript

Brain Behav Immun. Author manuscript; available in PMC 2017 August 01.

Published in final edited form as:

Brain Behav Immun. 2016 August ; 56: 378–389. doi:10.1016/j.bbi.2016.03.003.

Spinal activity of interleukin 6 mediates myelin basic protein-induced allodynia

Justin S. Ko[1,3], **Kelly A. Eddinger**[1], **Mila Angert**[1,2], **Andrei V. Chernov**[4], **Jennifer Dolkas**[1,2], **Alex Y. Strongin**[4], **Tony L. Yaksh**[1], and **Veronica I. Shubayev**[1,2,*]

[1]Department of Anesthesiology, University of California, San Diego, La Jolla, California, USA

[2]VA San Diego Healthcare System, La Jolla, California, USA

[3]Sungkyunkwan University School of Medicine, Samsung Medical Center, Seoul, South Korea

[4]Sanford-Burnham Prebys Medical Discovery Institute, La Jolla, California, USA

Abstract

Mechanosensory fibers are enveloped by myelin, a unique multilamellar membrane permitting salutatory neuronal conduction. Damage to myelin is thought to contribute to severe pain evoked by innocuous tactile stimulation (i.e. mechanical allodynia). Our earlier (Liu et al, *J. Neuroinflammation*, 9 (1): 119, 2012) and present data demonstrate that a single injection of a myelin basic protein-derived peptide (MBP84–104) into an intact sciatic nerve produces a robust and long-lasting (>30 days) mechanical allodynia in female rats. The MBP84-104 peptide represents the immunodominant epitope and requires T cells to maintain allodynia. Surprisingly, only systemic gabapentin (a ligand of voltage-gated calcium channel α2δ1), but not ketorolac (COX inhibitor), lidocaine (sodium channel blocker) or MK801 (NMDA antagonist) reverse allodynia induced by the intrasciatic MBP84-104. The genome-wide transcriptional profiling of the sciatic nerve followed by the bioinformatics analyses of the expression changes identified interleukin (IL)-6 as the major cytokine induced by MBP84-104 in both the control and athymic T cell-deficient nude rats. The intrasciatic MBP84-104 injection resulted in both unilateral allodynia and unilateral IL-6 increase the segmental spinal cord (neurons and astrocytes). An intrathecal delivery of a function-blocking IL-6 antibody reduced the allodynia in part by the transcriptional effects in large-diameter primary afferents in DRG. Our data suggest that MBP regulates IL-6 expression in the nervous system and that the spinal IL-6 activity mediates nociceptive processing

*Corresponding Author: Veronica I. Shubayev, Department of Anesthesiology, University of California San Diego, 9500 Gilman Drive, La Jolla, CA 92093-0629. Phone: (858) 534-5278; Fax: (858) 534-1445; vshubayev@ucsd.edu.

COMPETING INTERESTS: The authors declare no competing interests.

AUTHOR'S CONTRIBUTIONS: JSK and JD carried out animal procedures, immunostaining and image analyses; KAE carried out animal procedures and behavioral analyses; MA, JSK and VIS performed RT-PCR analyses; AVC carried out gene array and bioinformatics analyses; VIS, TYL, JSK and AYS conceptualized, designed and coordinated execution of the studies, and wrote the manuscript. All authors read and approved the final manuscript.

stimulated by the MBP epitopes released after damage or disease of the somatosensory nervous system.

1. INTRODUCTION

After injury to the peripheral nervous system (PNS), disruption of the myelin sheath and electrical insulation of mechanosensory Aβ afferents contribute to the pain behavior phenotype induced by innocuous stimuli (allodynia) [1–3]. The molecular events that engage non-nociceptive Aβ afferents in pain processing are just beginning to unfold. Antigen-specific adaptive immunity and T-helper (Th)1 and Th17 cell polarization promote neuropathic pain via a release of pro-inflammatory, algesic cytokines, such as interleukin (IL)-1β and IL-17, respectively [4–9]. Our recent findings implicate the proteolytic release of the cryptic Th cell epitopes of myelin basic protein (MBP) as a major event in the pathophysiology for mechanical allodynia after traumatic PNS injury [10].

Myelin basic protein (MBP), a major protein of the myelin sheath, is encoded by the *Golli (genes of oligodendrocyte lineage)-MBP* gene in myelinating glia and immune cells [11]. As an intrinsically unstructured and positively charged protein with the isoelectric point at ~pH 10, MBP interacts with the acidic head groups of the lipid bilayer and a variety of polyanionic proteins, including actin, tubulin and Ca^{2+}-calmodulin. These interactions regulate multiple functions of the axon-glia unit, including cytoskeletal assembly, Ca^{2+} homeostasis and a protein:lipid ratio in the myelin membranes [11, 12]. However, the centrally located cryptic MBP epitopes (e.g. MBP84-104), when released by proteolysis, are encephalitogenic in patients with multiple sclerosis and experimental autoimmune encephalomyelitis (EAE) animals [11]. According to our observations, a localized injection of the MBP84-104 peptide into the intact PNS (sciatic nerve) is sufficient to initiate a molecular cascade leading to robust mechanical allodynia in rats [10]. Because T cell activity is required mainly for the maintenance of MBP84-104-induced allodynia, as athymic nude rats initially develop mild mechanical hypersensitivity after MBP84-104 injection [10], and T cells are among the last immune cell type to infiltrate the PNS injury [13], the early algesic mechanisms of the MBP84-104 action, preceding or independent of T cell recruitment, remain obscure.

IL-6 (or interferon β2) is a pleiotropic cytokine with a plethora of regulatory functions [14–16], including the transition of innate to adaptive immunity [17]. In the nervous system, immune cells glia and neurons produce IL-6 to regulate a wide range of physiological and pathological events [14, 18, 19]. In EAE, IL-6 mediates T cell recruitment and subsequent Th17 polarization [20, 21], suggesting that IL-6 activity may also precede and facilitate the algesic T cell activity induced by MBP epitope release or injection in the PNS. Accordingly, IL-6 causes robust mechanical allodynia [22] following intraplantar [23], intrathecal [24] or intracerebroventricular [25] injections, and increase in the IL-6 expression after PNS injury has been implicated in the pathogenesis of experimental neuropathic pain [24, 26–33]. Consequently, a function-blocking IL-6 antibody delivered intrathecally, attenuates pain associated with spinal nerve ligation [31], sciatic nerve constriction [32] and ventral root transection [33].

Herein, we demonstrated that IL-6 at least partly mediated pain induced by MBP84-104 peptide. The bioinformatics analyses of our genome-wide transcriptional profiling of the sciatic nerves injected with MBP84-104 [10] identified IL-6 as the top-induced cytokine in both the athymic nude and control rat samples, independent of T cell content. Unilateral allodynia caused by the intrasciatic MBP84-104 injection was concomitant with the unilateral increase in the IL-6 expression in the segmental spinal cord. Interference with spinal IL-6 activity by intrathecally delivered function-blocking antibody reduced MBP84-104-induced allodynia, corroborating spinal IL-6 was positioned downstream of the pro-nociceptive MBP activity in neuropathic pain.

2. METHODS

2.1 Reagents and antibodies

Routine reagents were purchased from Sigma unless indicated otherwise. MBP84-104 (ENPVVHFFKNIVTPRTPPPSQ) and scrambled (s)MBP84-104 (NKPQTNVVEPFHRTFPIPPVS) peptides, derived from the human MBP sequence (GenBank #AAH08749), were synthesized by GenScript. The peptides were protected from degradation by exoproteinases using N-terminal acetylation and C-terminal amidation. The following primary antibodies were used in our immunofluorescence analyses: goat polyclonal IL-6 [R&D Systems (AF506), 1:100], goat polyclonal IL-6 receptor [IL-6R, R&D Systems (AF1830), 1:100], rabbit polyclonal glial fibrillary acidic protein [GFAP, DAKO (Z0334), 1:500], mouse monoclonal NeuN [EMD Millipore (MAB377), 1:1000], rabbit ionized Ca^{2+}-binding adapter molecule 1 [Iba1, Wako (019-19741), 1:500], mouse neurofilament 200 [NF200, Millipore (MAB5262), 1:200], rabbit polyclonal calcitonin gene-related peptide [CGRP, Abcam (ab47027), 1:400], and rabbit polyclonal activating transcription factor 3 [ATF3, C-19 clone, Santa Cruz Biotechnology (SC-188), 1:100].

2.2 Animal models

Female Sprague-Dawley rats (200–225 g), athymic nude rats (Hsd:RH-*Foxn1*^{rnu}, 8-week-old) and their heterozygous controls (Hsd:RH-*Foxn1*^{rnu}/*Foxn1*$^{+}$, 8-week-old, n=6) were obtained from Harlan Labs and housed in a temperature-controlled room (~22 °C), on a 12-h light/dark cycle with free access to food and water. All the procedure and testing were conducted during the light cycle. Under isoflurane anesthesia, the common sciatic nerve was exposed unilaterally at the mid-thigh level. A single intrasciatic (IS) bolus injection of the MBP84-104 and sMBP84-104 peptides (50 μg in 5 μl PBS each) was performed into the nerve fascicle using a 33-gauge needle on a Hamilton syringe. In a subset of animals, the exposed sciatic nerve received three loosely constrictive chromic gut ligatures to produce chronic constriction injury (CCI) [34]. Sciatic nerve, lumbar (L)4–5 dorsal root ganglia (DRG) and L1–L6 spinal cords were excised and stored in RNA-later (Ambion) at −20° C for RNA analyses, or in animals perfused with 4% paraformaldehyde, the excised tissues were post-fixed and cryoprotected in graded sucrose for immunochemistry. Tissues from naïve animals were used as control. Animals were sacrificed using Beuthanasia IP (Schering-Plough Animal Health). All animal procedures were performed according to the PHS Policy on Humane Care and Use of Laboratory Animals with the experimental protocol approved by the Institutional Animal Care and Use Committee at the University of

California, San Diego and VA San Diego Healthcare System, and complied with ethical guidelines of the International Association for the Study of Pain.

2.3 Behavior tests

Animals were habituated to the testing environment prior to baseline tests. Testing was performed daily for three consecutive days prior and then daily after a single IS MBP84-104 and sMBP84-104 injection. For assessment of *mechanical withdrawal threshold*, rats were placed in individual Plexiglas compartments with wire mesh bottom and von Frey filaments (0.41–15.2 g, Stoelting, Wood Dale, IL, USA) were applied perpendicularly to the mid hind paw and held for 4–6 s. A positive response was noted if the paw was sharply withdrawn. The 50% probability of withdrawal threshold was determined by Dixon's up-down method [35]. To assess *thermal escape latencies*, a modified Hargreaves type device was employed [36]. Rats were placed individually in Plexiglas cubicles with glass surface and, after habituation, a radiant heat stimulus was applied to each paw and the latency defined as the time (seconds) required for the paw to show a brisk withdrawal.

2.4 Drug delivery

The drugs were delivered at day 7 after a single IS MBP84-104 injection. To allow intrathecal (IT) delivery, chronic lumbar IT catheters, single-lumen polyethylene (OD 0.36 mm, 8.5 cm in length), were implanted under isoflurane anesthesia [37]. The function-blocking goat antibody against rat IL-6 (R&D Systems, AF506)) or normal goat IgG (R&D Systems, AB-108-C) was administered IT (50 ng each in 10 μl saline), followed by 10 μl saline (0.9% NaCl) flush. Gabapentin (Toronto Research Chemicals, G117250, 200 mg/kg), ketorolac (Sigma Aldrich, K1136, 30 mg/kg), MK801 (Sigma Aldrich, M107, 0.05 mg/kg) and lidocaine (Sigma Aldrich, L5647, 2 mg/kg) were each administered by intraperitoneal (IP) injection in 0.9% NaCl (2 ml/kg).

2.5 *Taqman* qRT-PCR

Total RNA was extracted using TRIzol (Invitrogen) and purified on an RNeasy mini column (Qiagen). The RNA purity was estimated by measuring the OD260/280 ratio. The integrity of the RNA samples was validated using an Experion automated electrophoresis system (Bio-Rad). The samples were treated with RNase-free DNAse I (Qiagen). cDNA was synthesized using a SuperScript first-strand RT-PCR kit (Invitrogen). Real-time RT-PCR was conducted using Mx3005P™ qPCR System (Agilent) in 25 μl reactions containing *Taqman* Universal PCR Master Mix (Ambion), cDNA (50 ng), specific forward and reverse primers (900 nM each) and *Taqman* probes (200–300 nM), specified in Table 1, with a one-step program: 95°C, 10 min; 95°C, 30 sec; 60°C, 1 min for 50 cycles. Duplicate samples without cDNA (a no template control) showed no contaminating DNA. Normalization to glyceraldehyde 3-phosphate dehydrogenase (GAPDH) and relative mRNA quantification were performed in MBP84-104- and sMBP84-104 sample groups and calibrated to naïve samples using the 2(−Delta Delta C(T)) method [38]. The fold-change calculations were performed using MxPro qPCR software (Agilent), as described [39].

2.6 Genome-wide transcriptome and pathway analyses

The samples of total RNA (50 ng) from the athymic nude and control rat sciatic nerves were labeled using a LowInput QuickAmp Labeling Kit and Cy3-CTP (Agilent). The labeled RNA samples were hybridized for 17 h at 65°C to SurePrint G3 Rat GE 8x60K slides (Agilent). Slides were scanned using an Agilent C Scanner. The raw data were processed using Feature Extraction software version 10.5. The initial analysis and normalization to the median were performed using GeneSpring GX software (Agilent). Differentially expressed mRNAs with signal intensities higher than two-fold over the background standard deviation were filtered by t-test. The statistically significant data ($p \leq 0.05$) were used to calculate gene expression ratios in the samples. The gene expression data were deposited to GEO database (accession # GSE34868). Functional clustering was conducted using Ingenuity Pathway Analyses (Qiagen). The association of genes with biological functions and canonical pathways was based on the respective p-values, calculated using the right-tailed Fisher exact test [40].

2.7 Immunohistochemistry

In cryoprotected and Optimal Cutting Temperature (OCT)-embedded, 4% paraformaldehyde-fixed tissues sections (10 μm), non-specific binding was blocked using 5% donkey serum in 0.3% Triton X-100 for 30 min at ambient temperature. The sections were incubated with a primary antibody (16–18 h at 4°C) followed by the species-specific Alexa 488-conjugated secondary antibody (green, Molecular Probes, 1 h, ambient temperature), and then a second primary antibody (16–18 h at 4°C), followed by the species-specific Alexa 594-conjugated secondary antibody (red, Molecular Probes, 1 h, ambient temperature). The sections were rinsed in PBS. The nuclei were stained with DAPI (4′,6-diamidino-2-phenylindole, Molecular Probes, blue). The absence of non-specific staining was confirmed by omission of a primary antibody or using a non-immune serum. Sections were mounted using a Slowfade Gold antifade reagent (Molecular Probes). The images were acquired using a Leica DMR microscope and Openlab 4.04 imaging software (Improvision), using equal parameters (digital gain, maximum white level, exposure time, and black level) for the experimental and control groups.

2.8 Data analyses

Statistical analyses were performed using GraphPrism 4.03 (Synergy Software) or SPSS 16.0 (SPSS) software by a two-tailed, unpaired Student's t-test for comparing two groups, or analyses of variance (ANOVA) for repeated measures for comparing three or more groups, followed by the Bonferroni or Tukey-Kramer post-hoc test, unless specified otherwise. $p \leq 0.05$ values were considered significant.

3. RESULTS

3.1 Sustained MBP-induced mechanical allodynia is reversed by gabapentin

Animals received a single IS bolus injection of MBP84-104 or sMBP84-104, followed by von Frey and then Hargreaves tests in the same animal cohort. The paw withdrawal thresholds to von Frey hair stimulation (Fig. 1A) dropped by day 1 post-injection ($p \leq 0.05$)

and the robust mechanical allodynia continued for the 7-day testing period ($p \leq 0.01$) in the ipsilateral paw of rats treated with MBP84-104. In contrast, the scrambled peptide produced no tactile thresholds of less than 10 grams throughout the tested time-course. No contralateral changes in paw withdrawal threshold were observed following the injection with either peptide. Thermal escape latencies (Fig. 1B) and motor functions were not affected following IS MBP84-104 and sMBP84-104 injections in rats.

To determine if the MBP84-104-induced tactile allodynia was sensitive to known analgesic drugs, the representative compounds from the four different drug classes were administered systemically in rats once at day 7 after IS MBP84-104 injection: (a) gabapentin (200 mg/kg, IP), a ligand binding to the α2δ1 subunit of the voltage-gated Ca^{2+} channel [41]; (b) MK801 (0.05 mg/kg, IP), an N-methyl-D-aspartate (NMDA) receptor blocker [42]; (c) ketorolac (30 mg/kg, IP), a non steroidal mixed cyclooxygenase inhibiting anti-inflammatory drug [43]; and (d) lidocaine (2 mg/kg, IP), a sodium channel blocker (Fig. 1C). The IS injection of MBP84-104 resulted in tactile allodynia sustained for 7 days, as apparent by baselines of ~2–3 grams (as compared to ~13 grams in the control rats, Fig. 1A). At day 7 post-IS MBP84-104, gabapentin therapy resulted in a transient reversal of the allodynia, which lasted for about 4 h, the typical duration of gabapentin action in the rat. No other drug tested, including MK801, ketorolac and lidocaine, administered either IP (Fig. 1C), or IT MK801 (0.05 mg/kg ≈ 10 μg/10μL, data not shown), produced any significant analgesic effect.

To assess the long-term effects of IS MBP-84-104, von Frey testing was performed at days 3, 5, 11, 18, 20, 27 and 32 post-injection of in a group of additional 10 rats (Fig. 1D). As expected, the paw withdrawal thresholds dropped within day 1 post-injection and in a majority of the animal cohort (n=9 out of 10), it remained below the threshold of 5 gram force for at least 11 days after a single IS bolus injection ($p \leq 0.01$). By day 30 post-injection, 30% of animals (n=3 out of 10) continued to display severe allodynia (subgroup I), one animal maintained mechanical hypersensitivity and a larger animal cohort (n=6 out 10) gradually reached the baseline of ~15 gram force (subgroup II).

Together, these data demonstrate that IS MBP84-104 is sufficient to initiate a robust unilateral and selective mechanical, but not thermal/heat pain hypersensitivity in females, sustained for up to 30 days and resistant to conventional analgesic therapy, except for gabapentin.

3.2 IL-6 is the major cytokine induced by MBP84-104, regardless of T cell content

In athymic nude (Hsd:RH-*Foxn1*^{rnu}) rats, the *rnu* allele is an autosomal recessive mutation associated with hairlessness and thymic aplasia causing T cell depletion. To determine if T cells are linked to the MBP84-104-induced induction of IL-6, we performed comparative genome-wide transcriptional profiling of sciatic nerve samples obtained from athymic nude rats and their heterozygous controls. Rats received IS MBP84-104. At day 7 post-injection the samples were collected, total RNA was isolated from the samples and then the levels of the respective mRNAs were assessed using a rat gene array. The analysis of the expression data dataset (GEO accession #GSE34868) [10] suggested that IL-6 was one of the top genes induced by the MBP84-104 injection, in rat sciatic nerve in both athymic and especially control animals (4.5- and 11.6-fold increase, respectively). The up-regulation of IL-6 relative

to other cytokines was highlighted by using the Ingenuity analysis of the *Role of Cytokines in Mediating Communication between Cells* signaling pathway in the gene profiling datasets (Fig. 2). As compared with IL-6, the level of induction of additional cytokines and growth factors (IL-1β, IL-10, IL-3, IL-8, TNF-α, GCSF, INF-γ) in the nerve samples of nude and their control rats was less significant or nonexistent. We concluded that MBP84-104 was a potent inducer of IL-6 in the nervous system, and that the MBP84-104 ability to induce IL-6 did not depend on the T cell function.

In the absence of T cells, the *rnu* rat strain, backcrossed into eight inbred rat strains, maintains the normal complement of B cells, yet elevated NK1 cell populations. Thus, we next sought to confirm the changes in IL-6 in the Sprague-Dawley rat strain used in the rest of the study.

3.3 Unilateral increase in IL-6 expression in the spinal cord after IS MBP

In the tissues obtained from the Sprague-Dawley rats at day 7 after IS MBP84-104 or sMBP84-104 injections following daily behavioral testing (Fig 1A–B), we measured the levels of IL-6 and other inflammatory mediators (IL-1β, IL-10, TNF-α and Arg-1) using *Taqman* qRT-PCR. The samples were obtained from the nerve segments at the peptide injection site, the segmental DRG and the segmental spinal cord, as illustrated in Fig 3A.

At the nerve injection site, the IL-6 mRNA expression increased 2.5-fold at day 7 after MBP84-104 injection relative to naïve nerve (Fig 3B). There was no increase observed in the nerve samples of animals that receive the scrambled peptide (0.8-fold relative to the naïve), yet the difference between the effects of MBP84-104 and sMBP84-104 was not statistically significant ($p>0.05$). In comparison, in the nerve samples obtained at day 7 post-CCI IL-6 levels increased 93-fold versus the naïve nerve samples ($p<0.05$).

In the ipsilateral DRG, the IL-6 mRNA expression also increased at day 7 after MBP84-104 injection (4.2-fold) relative to naïve DRG samples (Fig 3B). The increase in IL-6 in the ipsilateral sMBP84-104 DRG was less evident (2.9-fold) relative to naïve DRG, but not statistically significant from the MBP84-104 DRG samples ($p>0.05$). A significant ($p<0.05$) 58-fold increase in IL-6 was recorded in the DRG samples at day 7 after CCI relative to naïve DRG.

In the ipsilateral spinal cord (dorsal quarter), the IL-6 mRNA expression increased 28.6-fold at day 7 after MBP84-104 injection compared to the corresponding naïve spinal cord (Fig. 3B). In turn, IL-6 decreased in the respective sMBP84-104 samples (0.5-fold) suggesting the presence of an over 58-fold difference in the level of IL-6 in the MBP84-104 versus the sMBP84-104 spinal cord samples ($p<0.05$). In a similar manner, we recorded a significant 276-fold increase in the IL-6 mRNA at day 7 post-CCI in the ipsilateral dorsal spinal cord as compared with the naïve control.

In the contralateral nerve and DRG samples, the expression of IL-6 mildly declined in both the MBP84-104 and sMBP84-104 samples relative to the corresponding naïve samples, although the changes were not statistically significant ($p>0.05$). Likewise, no significant difference in the IL-6 mRNA was observed in the contralateral dorsal spinal cord after IS

MBP84-104 and sMBP84-104 injection (3.0-fold and 1.67-fold compared to naïve samples, respectively, $p>0.05$). It is worth noting that IL-6 expression is relatively low, albeit readily detectable in naïve nerve, DRG and spinal cord samples, as evident by the threshold cycle (Ct) of amplification for IL-6 (32–34) and normalizer *GAPDH* (18–22).

To determine if the IS MBP-84-104-induced long-term allodynia correlated with levels of IL-6 in the spinal cord, at the end of the behavior testing (day 32, Fig. 1D), the expression of IL-6 mRNA in the spinal cord (dorsal quarter) was assessed in the subgroup I (sustained pain) and subgroup II (no sustained pain) samples. Interestingly, IL-6 expression was slightly below that measured in the naïve spinal cord ($p>0.05$) corresponding to a 0.3-fold and 0.69-fold increase in subgroups I and II, respectively, thus no longer correlating with the pain-like behavior.

In contrast to IL-6, the changes in IL-1β, IL-10, TNF-α and Arg-1 mRNA expression were not significantly different between MBP84-104 or sMBP84-104 groups in any of the analyzed tissues at day 7 or 32 post-injection (data not shown). Because if compared to the scrambled peptide, IS MBP84-104 peptide caused the unilateral induction of the spinal IL-6 synthesis and the unilateral allodynia at day 7 post-injection, we sought to assess the effect of spinal IL-6 blockade on the MBP84-104-induced allodynia at this time-point next.

3.4 Inhibition of the spinal IL-6 activity attenuates allodynia after IS MBP

The function-blocking IL-6 antibody, intrathecally delivered, attenuates pain after various types of injury [31¯33]. Thus, at day 7 after a single IS bolus injection of MBP84-104 and established mechanical allodynia in the ipsilateral paw ($p\leq0.05$, Fig. 4A), the function-blocking IL-6 antibody (5 ng/μl, 10 μl) or control normal IgG (5 ng/μl, 10 μl) were administered IT.

Delivery of the IL-6-blocking antibody resulted in an increase in tactile thresholds (i.e., a reduction in the tactile allodynia) that was statistically significant at the first testing point and this reversal continued to increase over the next three days (Fig. 4A). IL-6-blocking demonstrated apparent efficacy in strongly significantly reducing the MBP-induced allodynia. By day 10 the reversal, while significant, was incomplete. This may reflect on the pharmacokinetics of the antibody in reaching the target (and a complete reversal might have been noted had a longer time been allowed to elapse) or a hysteresis in the mechanisms that are being reversed. In contrast, the control IgG produced no effect (Fig. 4A). However, the IL-6-blocking antibody was ineffective when administered IT 30 min prior to IS MBP84-104 (data not shown). There were no contralateral effects recorded after the IT administration of the IL-6-blocking antibody or IgG control IT 30 min prior or 7 days after IS MBP84-104 injection (data not shown).

Following the behavioral tests, the ipsilateral DRG and the spinal cord (the dorsal quarter) samples were subjected to the *Taqman* qRT-PCR analysis for ATF3 gene, as the intraganglionic PNS injury marker expressed mainly by large-diameter neurons [44], and Cacna2d1 encoding voltage-gated Ca^{2+} channel, α2δ1 subunit 1 [45]. The IS MBP84-104 induced a 4.82-fold and 3.14-fold increase in ATF3 in DRG in the IgG control and IL-6 antibody groups, respectively, compared with naïve DRG (Fig. 4C). The IS MBP84-104

induced a 1.82-fold (82%) and 1.32-fold (32%) increase in Cacna2d1 in DRG in the IgG control and IL-6 antibody groups, respectively, compared with naïve DRG, corresponding to the significant ($p<0.05$) decline in both genes after IL-6 blockade compared with the IgG control. It is important to point out that baseline expression of Cacna2d1 was relatively high in naïve DRG (Ct of 6 cycles above GAPDH). In the dorsal spinal cord, in contrast to the CCI, there were no statistically significant changes recorded in the expression of Cacna2d1, ATF3, and toll-like receptor-4 (by qRT-PCR) or GFAP (by immunoreactivity) after IS MBP84-104 with or without IL-6 inhibition compared with the IgG control (data not shown). We concluded that IT IL-6-neutralizing therapy may act to inhibit MBP84-104-induced pain at least in part through transcriptional changes in the primary afferent DRG neurons.

Because functional activity of IL-6 in nociceptive processing depends on IL-6R, which binds to ubiquitously expressed glycoprotein (gp)130 [14, 22], IL-6R immunoreactivity was assessed in the ipsilateral DRG neurons 7 days after the IS MBP84-104 injection. Consistent with the transcriptional DRG changes after IT IL-6 blockade, large-diameter DRG neurons, including ATF3+ neurons, and the supporting GFAP-positive satellite glia express IL-6R after IS MBP84-104 (Fig. 4D) similarly to PNS injury [46].

3.5 Identification of cells producing IL-6 in nerve, DRG and spinal cord after IS MBP

T cell deficiency did not significantly affect the IL-6 synthesis in response to IS MBP84-104 (Fig. 2). To identify the cell types responsible for the IL-6 synthesis along the MBP84-104-injected neural axis, we performed immunostaining of IL-6 and the relevant cell markers in the ipsilateral nerve, DRG and spinal cord samples obtained from rats at day 7 after MBP84-104 or scrambled peptide injection. In agreement with the RT-PCR data, the IL-6 immunoreactivity was detecteble in naïve nerve and even more pronounced at the site of MBP84-104 injection. Myelinating Schwann cells (identified by their distinct crescent shape resulting from their 1:1 association with axons) and the Iba1-positive macrophages were the main cell types producing IL-6 (Fig. 5B). Furthermore, the number of Iba1-positive macrophages were increased in MBP84-104 nerve samples (Appendix 1).

In the ipsilateral DRG samples, the immunoreactivity of IL-6 was readily observed at day 7 of IS MBP84-104 injection and to the lesser degree, the sMBP84-104 or naïve DRGs (Fig. 6A). According to the IL-6 dual-labeling with cell specific markers, certain NF200-positive (A-type) and CGRP-positive (C-type) neurons, as well as GFAP-positive satellite cells produced IL-6 in the DRG ipsilateral to IS MBP84-104 injection (Fig. 6B). The contribution of the Iba1-positive macrophages to IL-6 production in the DRG was insignificant (Fig. 6B). The effect of IS MBP84-104 on the Iba1-positive numbers in the DRG was modest as compared with that of sMBP84-104 (Appendix 1).

In the ipsilateral dorsal horn of spinal cord, IL-6 immunoreactivity was observed at day 7 after IS MBP84-104 injection, and to a lesser degree, after scrambled peptide injection and naïve cords (Fig. 7A). The IL-6 immunoreactivity localized in many neurons, as confirmed using NeuN, including some pro-nociceptive, CGRP-positive neurons (Fig. 7B). In addition, GFAP-positive astrocytes were a major source of IL-6 in the spinal cord of the MBP84-104-injected rats. The GFAP immunoreactivity pattern also indicated the development of spinal

astrogliosis in rats at day 7 after IS MBP84-104 injection as compared with rats treated with the scrambled peptide (Appendix 1). In contrast, Iba1-positive microglia appeared only occasionally IL-6-reactive (Fig. 7B) and insignificantly activated in the spinal cord after IS MBP84-104 injection (Appendix 1).

4. DISCUSSION

In this study, we observed that intrasciatic injection of immunodominant MBP peptide into an intact nerve produced robust and sustained mechanical allodynia. We believe that this effect is mediated in part by stimulating spinal expression of the algesic cytokine, IL-6 (interferon β2). Accordingly, intrathecally delivered IL-6-blocking therapy reduced MBP-induced pain. In addition, gabapentin, but not ketolorac, MK801 or lidocaine, was efficacious against MBP-induced pain.

4.1 MBP and pain: Clinical implications

Mechanical allodynia is a common sequelae of afferent/neuraxial lesions and neurodegenerative or neuroinflammatory states. It has become apparent that large-diameter mechanosensory Aβ afferents, involved in nociception only after PNS injury, and their unique structures, such as myelin sheath, contribute to mechanical allodynia [1–3, 47–49]. As in the present preclinical work, the clinical pain associated with many of these conditions is often refractory to common analgesics [50]. In our present and previous reports, we provide the first evidence that the myelin auto-antigens are released after PNS trauma [10, 47] and when injected into an intact PNS as pure peptides are sufficient to induce robust, selective and long-lasting mechanical pain hypersensitivity without affecting basal nociception (heat sensitivity) or motor functions.

MBP69-86 and MBP84-104, are major peptidic auto-antigens present in in Guillain-Barre syndrome and in multiple sclerosis [11]. Several observations have led us to hypothesize that these peptide epitopes play a pivotal role in nociceptive processing following nerve injury: i) Our unbiased bioinformatics analyses suggesting the sciatic CCI nerve proteome resembled pathogenesis of multiple sclerosis [10] led us to hypothesize a direct role of MBP as a pain mediator. ii) In models of peripheral mononeuropathy, e.g. CCI [10] and spinal nerve crush [47], we find the MBP epitope release, using a confirmation-specific antibody to the degraded MBP69-86 sequence (AB5864, Millipore). iii) Importantly, these peptide fragments are robustly pro-nociceptive [10]. Accordingly, we argue that release of the pro-nociceptive MBP peptides contributes to mechanical pain hypersensitivity associated with PNS injury. Given the presence of these peptide fragments in neurodegenerative disorders, we suggest the likelihood that their contribution to a neuropathic pain state will manifest in various clinical pain syndromes arising not only from peripheral nerve trauma or compression (e.g., due to entrapment or tumor). Since we recorded the pro-nociceptive MBP peptide release in the absence of widespread demyelination [10, 47], we believe it may contribute to a variety of idiopathic neuropathic pain conditions, including those arising from autoimmune demyelination (e.g., Guillain-Barre syndrome or multiple sclerosis), toxic syndromes (e.g., chemotherapy or alcohol), viral (e.g., HIV and HPV) pathogens or metabolic diseases (e.g. diabetes).

Therapeutic inhibition of the MBP epitope release using matrix metalloproteinase (MMP) inhibitors attenuates mechanical allodynia associated with CCI [10] and spinal nerve crush [47]. The observation that it is the centrally located, but not the N-terminal, MBP peptide sequences initiate allodynia [10] suggests a potential drug target. Thus, therapy using the central MBP-derived mutant/altered peptide ligand (APL) analogues, impair T cell function and alleviate mechanical allodynia associated with EAE [51] and CCI [52, 53]. Since our studies employ female rats, the MBP-induced T cell activation in nerve and spinal cord [10] is a plausible mechanism underlying the differential female versus male processing of mechanical pain hypersensitivity after PNS injury [7].

4.2 MBP, adaptive immunity and mechanical allodynia

We determined, using athymic nude rats, that T cells are required to sustain MBP-induced allodynia [10]. Generally, Th1 and Th17 cells expressing algesic cytokines sustain pain that follows PNS trauma, whereas Th2 and Treg cells expressing analgesic cytokines inhibit pain processing [4–6, 8, 9, 13, 54–58]. Evidence exists that persistent pain states involving nerve but not surrounding tissue damage activate adaptive immunity [59]. This provides support for the role of the injury to nerve-specific structures, such as myelin, in pain processing. Typically, major histocompatibility complex (MHC) class II presents the MBP epitopes on a surface of antigen-presenting macrophages and Schwann cells in the PNS [10, 60], and then the MBP•MHCII complex guides the T cell receptor binding [11, 12]. In agreement, MHCII is essential to the development of neuropathic pain after PNS injury [59]. In addition, B cells present the MBP epitopes via complement receptor (CR)2 [61].

T cell recruitment [20, 21] and Th17 polarization [62] both depend on IL-6 activity in EAE. Accordingly, we suggest that T cell recruitment and Th17 polarization after IS MBP84-104 [10] relate to the concomitant increase in IL-6 expression, which we find to be T cell-independent. Th17-released IL-17 enhances the glial IL-6 production resulting in a positive feedback loop [63], thereby augmenting further the IL-17 synthesis in Th17 cells [64, 65]. While systemic T cell activation, causing demyelination, is a likely cause of pain associated with EAE [51], direct IS administration of a pure MBP84-104 peptide into an intact nerve confirms that the activity of the MBP epitopes is sufficient to induce robust and lasting pain.

MBP84-104 selectively increases mechanical but not thermal (heat) pain hypersensitivity both in our present and earlier reports [10]. This specific effect upon mechanical sensitivity likely arises from changes in the afferent signaling in mechanically selective fibers, suggesting the involvement of low-threshold Aβ fibers [2, 48]. The absence of changes in thermal escape latencies or in the expression of the major inflammatory genes after IS MBP84-104, or the failure of COX inhibitors and other analgesics to attenuate MBP-induced allodynia, suggest that sensitization of C polymodal nociceptors is unlikely. Thus, MBP induces a robust pain state *without* widespread inflammation or involvement of conventional nociceptive circuitry. We have proposed a model [10] whereby selective mechanical pain hypersensitivity is caused by a localized release of myelin-specific auto-antigens, including but not limited to MBP, in myelinated (i.e. mechanosensitive A-afferent) fibers, thus sparing unmyelinated (i.e., heat-sensitive C-afferent) fibers from Th1/17 cell homing. In agreement, deficiency in the algesic IL-17, released by Th17, selectively protects from mechanical

allodynia and not thermal hyperalgesia following nerve trauma [8]. This model, however, does not explain the lack of myelinated efferent involvement as judged by lack of motor abnormalities after IS MBP84-104.

4.3 IS MBP84-104 induced IL-6 and pain processing

The MBP84-104 peptide induced IL-6 expression in the nervous system without causing a widespread inflammatory response. This data is consistent with the model of the cytokine- and prostaglandin-independent regulation of IL-6 synthesis [22]. Likewise, phosphorylated MBP has been shown to regulate IL-6 expression in B cells [66], and the full–length MBP induces IL-6 synthesis in endothelial cells [67]. In addition, the myelin debris stimulates IL-6 expression and the CR3-dependent NFkB activation in macrophages [68]. Although the mechanisms of MBP regulation in neurons or glia remain to be established, MBP is known to bind αMβ2 integrin/CD11b to activate PI3K signaling in other systems [69].

The levels of IL-6 expression after CCI exceed by several fold those recoded after IS MBP84-104, suggesting that factors additional to MBP contribute to IL-6 expression after PNS injury. In agreement with multiple models of PNS injury [24, 26–33], the early IL-6 expression after IS MBP84-104 is evident in nerve, DRG and spinal cord, lasting for over a week and gradually subsiding at later time-points. In that regards, IL-6 levels only partially correlate with pain-like behaviors [70]. In support of this conclusion, IL-6 levels were equally low in animals experiencing severe and no allodynia 1 month after IS MBP84-104. Conversely, nude rats exposed to IS MBP84-104 displayed high IL-6 levels yet minimal pain [10]. Since the IT blockade of IL-6 reduced, but did not prevent, MBP84-104-induced allodynia, the factors proximal to spinal IL-6 expression should contribute to its development.

IL-6 mediates nociceptive processing by stimulating substance P and prostaglandin synthesis [22–25], and intrathecally delivered IL-6 function-blocking antibody reduces pain after IS MBP84-104 and various types of PNS injury [31–33]. Likewise, the IL-6 gene deletion protects rodents from mechanical allodynia after nerve injury [71] and the intraplantar carrageenan injection [72]. Given the transient effect of IL-6 in chronic pain and beneficial functions in neuronal survival and regeneration [71, 73], we urge caution in selecting the effective therapeutic window for the IL-6/IL-6R targeting. Taken together, these findings suggest that the IL-6/IL-6R axis plays a role in the transition from acute-to-chronic pain state according to its role in the transition from innate-to-adaptive immunity [17].

4.4 Unilateral changes after IS MBP injection

IS MBP84-104 induced unilateral allodynia and unilateral IL-6 increased along the injected neuraxis and especially in the spinal cord. The IL-6 expression patterns after IS MBP84-104 are highly consistent with that observed in PNS injury models, apparent in endoneurial Schwann cells and macrophages [28, 74], DRG neurons and satellite cells [46], spinal neurons [24, 26] and spinal astrocytes [75]. In depth *in vitro* and *in vivo* analyses are necessary to establish the cells and mechanisms of MBP-induced IL-6 expression, especially in the remote sites. Similarly to PNS injury, IS MBP84-104 activated the *Adaptive Immune Pathways* and MHCII expression in the spinal cord [10, 59]. How the peripheral changes in

large afferent function post-IS MBP84-104 lead to a sustained pain state in response to low threshold mechanical stimuli remains obscure, particularly given the intrinsic inhibition of A-afferents in the dorsal horn. Although broad degenerative changes in MBP84-104 injected nerves are absent [10] and the major pro-inflammatory cytokine expression is unchanged relative to the scrambled peptide, their role in MBP-induced allodynia cannot be ruled out. Increase in IL-6 expression and the satellite cell activation suggest a trophic response in DRG at least partly comparable to PNS injury. In that regards, given the reported coupling of DRG neuronal soma with satellite cells via gap junctions [76–78], it will be interesting to assess the role of DRG gap junctions in the MBP84-104-induced allodynia.

4.5 T cell-independent role of MBP in Ca^{2+} signaling and pain

MBP displays direct neuron-specific (but not glial) toxicity *in vitro,* which seems to depend on its binding to sialic acid-containing lipids on the neuronal surface and regulation of the nonselective cation flow [79, 80]. Both in the presence and absence of T cells, IS MBP84-104 induces IL-6 and spinal Ca^{2+} signaling [10]. Accordingly, gabapentin reverses MBP84-104-induced pain, by binding voltage-gated Ca^{2+} channel α2δ1 [81]. MBP has also been shown to regulate activity of voltage-gated Ca^{2+} channel and Ca^{2+} flux in oligodendrocytes [82, 83] via a binding to Ca^{2+}-calmodulin [11]. Through the activity of Ca^{2+}-calmodulin-dependent protein kinase, α2δ1 controls IL-6 expression in neurons [84]. It is therefore conceivable that IL-6 mediates MBP-induced nociceptive processing by regulating the neuronal α2δ1 expression, observed here, and Ca^{2+}-related excitotoxicity [14].

Supplementary Material

Refer to Web version on PubMed Central for supplementary material.

Acknowledgments

National Institutes of Health RO1DE022757 (to VIS, TLY, AYS) and the Department of Veterans Affairs Merit Review Award (to VIS) supported this study.

References

1. Wu G, et al. Degeneration of myelinated efferent fibers induces spontaneous activity in uninjured C-fiber afferents. J Neurosci. 2002; 22(17):7746–53. [PubMed: 12196598]
2. Devor M. Ectopic discharge in Abeta afferents as a source of neuropathic pain. Exp Brain Res. 2009; 196(1):115–28. [PubMed: 19242687]
3. Zhu YL, et al. Early demyelination of primary A-fibers induces a rapid-onset of neuropathic pain in rat. Neuroscience. 2012; 200:186–98. [PubMed: 22061425]
4. Moalem G, Xu K, Yu L. T lymphocytes play a role in neuropathic pain following peripheral nerve injury in rats. Neuroscience. 2004; 129(3):767–77. [PubMed: 15541898]
5. Costigan M, et al. T-cell infiltration and signaling in the adult dorsal spinal cord is a major contributor to neuropathic pain-like hypersensitivity. J Neurosci. 2009; 29(46):14415–22. [PubMed: 19923276]
6. Cao L, DeLeo JA. CNS-infiltrating CD4+ T lymphocytes contribute to murine spinal nerve transection-induced neuropathic pain. Eur J Immunol. 2008; 38(2):448–58. [PubMed: 18196515]
7. Sorge RE, et al. Different immune cells mediate mechanical pain hypersensitivity in male and female mice. Nat Neurosci. 2015; 18(8):1081–3. [PubMed: 26120961]

8. Kim CF, Moalem-Taylor G. Interleukin-17 contributes to neuroinflammation and neuropathic pain following peripheral nerve injury in mice. J Pain. 2011; 12(3):370–83. [PubMed: 20889388]
9. Kleinschnitz C, et al. T cell infiltration after chronic constriction injury of mouse sciatic nerve is associated with interleukin-17 expression. Exp Neurol. 2006; 200(2):480–5. [PubMed: 16674943]
10. Liu H, et al. Immunodominant fragments of myelin basic protein initiate T cell-dependent pain. J Neuroinflammation. 2012; 9:119. [PubMed: 22676642]
11. Boggs JM. Myelin basic protein: a multifunctional protein. Cell Mol Life Sci. 2006; 63(17):1945–61. [PubMed: 16794783]
12. Harauz G, Boggs JM. Myelin management by the 18.5-kDa and 21.5-kDa classic myelin basic protein isoforms. J Neurochem. 2013; 125(3):334–61. [PubMed: 23398367]
13. Kim CF, Moalem-Taylor G. Detailed characterization of neuro-immune responses following neuropathic injury in mice. Brain Res. 2011; 1405:95–108. [PubMed: 21741621]
14. Spooren A, et al. Interleukin-6, a mental cytokine. Brain Res Rev. 2011; 67(1–2):157–83. [PubMed: 21238488]
15. Taga T, Kishimoto T. Gp130 and the interleukin-6 family of cytokines. Annu Rev Immunol. 1997; 15:797–819. [PubMed: 9143707]
16. Van Snick J. Interleukin-6: an overview. Annu Rev Immunol. 1990; 8:253–78. [PubMed: 2188664]
17. Jones SA. Directing transition from innate to acquired immunity: defining a role for IL-6. J Immunol. 2005; 175(6):3463–8. [PubMed: 16148087]
18. Gadient RA, Otten U. Identification of interleukin-6 (IL-6)-expressing neurons in the cerebellum and hippocampus of normal adult rats. Neurosci Lett. 1994; 182(2):243–6. [PubMed: 7715819]
19. Gijbels K, et al. Interleukin 6 production in the central nervous system during experimental autoimmune encephalomyelitis. Eur J Immunol. 1990; 20(1):233–5. [PubMed: 2307176]
20. Eugster HP, et al. IL-6-deficient mice resist myelin oligodendrocyte glycoprotein-induced autoimmune encephalomyelitis. Eur J Immunol. 1998; 28(7):2178–87. [PubMed: 9692887]
21. Serada S, et al. IL-6 blockade inhibits the induction of myelin antigen-specific Th17 cells and Th1 cells in experimental autoimmune encephalomyelitis. Proc Natl Acad Sci U S A. 2008; 105(26): 9041–6. [PubMed: 18577591]
22. De Jongh RF, et al. The role of interleukin-6 in nociception and pain. Anesth Analg. 2003; 96(4): 1096–103. table of contents. [PubMed: 12651667]
23. Cunha FQ, et al. The pivotal role of tumour necrosis factor alpha in the development of inflammatory hyperalgesia. Br J Pharmacol. 1992; 107(3):660–4. [PubMed: 1472964]
24. DeLeo JA, et al. Interleukin-6-mediated hyperalgesia/allodynia and increased spinal IL-6 expression in a rat mononeuropathy model. J Interferon Cytokine Res. 1996; 16(9):695–700. [PubMed: 8887053]
25. Oka T, et al. Intracerebroventricular injection of interleukin-6 induces thermal hyperalgesia in rats. Brain Res. 1995; 692(1–2):123–8. [PubMed: 8548295]
26. Arruda JL, et al. Increase of interleukin-6 mRNA in the spinal cord following peripheral nerve injury in the rat: potential role of IL-6 in neuropathic pain. Brain Res Mol Brain Res. 1998; 62(2): 228–35. [PubMed: 9813345]
27. Bourde O, et al. Quantification of interleukin-6 mRNA in wallerian degeneration by competitive reverse transcription polymerase chain reaction. J Neuroimmunol. 1996; 69(1–2):135–40. [PubMed: 8823385]
28. Kurek JB, et al. Up-regulation of leukaemia inhibitory factor and interleukin-6 in transected sciatic nerve and muscle following denervation. Neuromuscul Disord. 1996; 6(2):105–14. [PubMed: 8664561]
29. Murphy PG, et al. Induction of interleukin-6 in axotomized sensory neurons. J Neurosci. 1995; 15(7 Pt 2):5130–8. [PubMed: 7623140]
30. Chernov AV, et al. Calcium-binding proteins S100A8 and S100A9 initiate the early inflammatory program in injured peripheral nerve. The Journal of biological chemistry. 2015
31. Arruda JL, et al. Intrathecal anti-IL-6 antibody and IgG attenuates peripheral nerve injury-induced mechanical allodynia in the rat: possible immune modulation in neuropathic pain. Brain Res. 2000; 879(1–2):216–25. [PubMed: 11011025]

32. Lee KM, Jeon SM, Cho HJ. Tumor necrosis factor receptor 1 induces interleukin-6 upregulation through NF-kappaB in a rat neuropathic pain model. Eur J Pain. 2009; 13(8):794–806. [PubMed: 18938092]
33. Wei XH, et al. The up-regulation of IL-6 in DRG and spinal dorsal horn contributes to neuropathic pain following L5 ventral root transection. Exp Neurol. 2013; 241:159–68. [PubMed: 23261764]
34. Bennett GJ, Xie YK. A peripheral mononeuropathy in rat that produces disorders of pain sensation like those seen in man. Pain. 1988; 33(1):87–107. [PubMed: 2837713]
35. Chaplan SR, et al. Quantitative assessment of tactile allodynia in the rat paw. J Neurosci Methods. 1994; 53(1):55–63. [PubMed: 7990513]
36. Hargreaves K, et al. A new and sensitive method for measuring thermal nociception in cutaneous hyperalgesia. Pain. 1988; 32(1):77–88. [PubMed: 3340425]
37. Malkmus SA, Yaksh TL. Intrathecal catheterization and drug delivery in the rat. Methods Mol Med. 2004; 99:109–21. [PubMed: 15131333]
38. Livak KJ, Schmittgen TD. Analysis of relative gene expression data using real-time quantitative PCR and the 2(−Delta Delta C(T)) Method. Methods. 2001; 25(4):402–8. [PubMed: 11846609]
39. Pfaffl MW. A new mathematical model for relative quantification in real-time RT-PCR. Nucleic Acids Res. 2001; 29(9):e45. [PubMed: 11328886]
40. Chernov AV, et al. Microarray-based transcriptional and epigenetic profiling of matrix metalloproteinases, collagens, and related genes in cancer. J Biol Chem. 2010; 285(25):19647–59. [PubMed: 20404328]
41. Blackburn-Munro G, Erichsen HK. Antiepileptics and the treatment of neuropathic pain: evidence from animal models. Curr Pharm Des. 2005; 11(23):2961–76. [PubMed: 16178756]
42. Coan EJ, Saywood W, Collingridge GL. MK-801 blocks NMDA receptor-mediated synaptic transmission and long term potentiation in rat hippocampal slices. Neurosci Lett. 1987; 80(1):111–4. [PubMed: 2821457]
43. Buckley MM, Brogden RN, Ketorolac. A review of its pharmacodynamic and pharmacokinetic properties, and therapeutic potential. Drugs. 1990; 39(1):86–109. [PubMed: 2178916]
44. Seijffers R, Mills CD, Woolf CJ. ATF3 increases the intrinsic growth state of DRG neurons to enhance peripheral nerve regeneration. J Neurosci. 2007; 27(30):7911–20. [PubMed: 17652582]
45. Tuchman M, et al. Central sensitization and Ca(V)alphadelta ligands in chronic pain syndromes: pathologic processes and pharmacologic effect. J Pain. 2010; 11(12):1241–9. [PubMed: 20472509]
46. Dubovy P, et al. Satellite glial cells express IL-6 and corresponding signal-transducing receptors in the dorsal root ganglia of rat neuropathic pain model. Neuron Glia Biol. 2010; 6(1):73–83. [PubMed: 20519054]
47. Kobayashi H, et al. MMPs initiate Schwann cell-mediated MBP degradation and mechanical nociception after nerve damage. Mol Cell Neurosci. 2008; 39(4):619–27. [PubMed: 18817874]
48. Djouhri L, Lawson SN. Abeta-fiber nociceptive primary afferent neurons: a review of incidence and properties in relation to other afferent A-fiber neurons in mammals. Brain Res Brain Res Rev. 2004; 46(2):131–45. [PubMed: 15464202]
49. Woolf CJ, Doubell TP. The pathophysiology of chronic pain--increased sensitivity to low threshold A beta-fibre inputs. Current opinion in neurobiology. 1994; 4(4):525–34. [PubMed: 7812141]
50. Treede RD, et al. Neuropathic pain: redefinition and a grading system for clinical and research purposes. Neurology. 2008; 70(18):1630–5. [PubMed: 18003941]
51. Tian DH, et al. Effects of vaccination with altered Peptide ligand on chronic pain in experimental autoimmune encephalomyelitis, an animal model of multiple sclerosis. Front Neurol. 2013; 4:168. [PubMed: 24194728]
52. Perera CJ, et al. Active immunization with myelin-derived altered peptide ligand reduces mechanical pain hypersensitivity following peripheral nerve injury. Journal of neuroinflammation. 2015; 12(1):28. [PubMed: 25885812]
53. Perera CJ, et al. Effects of active immunisation with myelin basic protein and myelin-derived altered peptide ligand on pain hypersensitivity and neuroinflammation. J Neuroimmunol. 2015; 286:59–70. [PubMed: 26298325]

54. Liu H, et al. The alternatively spliced fibronectin CS1 isoform regulates IL-17A levels and mechanical allodynia after peripheral nerve injury. J Neuroinflammation. 2015 in press.
55. Tsai YC, Won SJ. Effects of tramadol on T lymphocyte proliferation and natural killer cell activity in rats with sciatic constriction injury. Pain. 2001; 92(1–2):63–9. [PubMed: 11323127]
56. Sweitzer SM, et al. Focal peripheral nerve injury induces leukocyte trafficking into the central nervous system: potential relationship to neuropathic pain. Pain. 2002; 100(1–2):163–70. [PubMed: 12435469]
57. Liu H, et al. Immunodominant fragments of myelin basic protein initiate T cell-dependent pain. Journal of neuroinflammation. 2012; 9:119. [PubMed: 22676642]
58. Austin PJ, Moalem-Taylor G. The neuro-immune balance in neuropathic pain: involvement of inflammatory immune cells, immune-like glial cells and cytokines. J Neuroimmunol. 2010; 229(1–2):26–50. [PubMed: 20870295]
59. Sweitzer SM, et al. The differential role of spinal MHC class II and cellular adhesion molecules in peripheral inflammatory versus neuropathic pain in rodents. J Neuroimmunol. 2002; 125(1–2):82–93. [PubMed: 11960644]
60. Kieseier BC, Hartung HP, Wiendl H. Immune circuitry in the peripheral nervous system. Curr Opin Neurol. 2006; 19(5):437–45. [PubMed: 16969152]
61. Seamons A, Perchellet A, Goverman J. Endogenous myelin basic protein is presented in the periphery by both dendritic cells and resting B cells with different functional consequences. J Immunol. 2006; 177(4):2097–106. [PubMed: 16887968]
62. Bettelli E, et al. Reciprocal developmental pathways for the generation of pathogenic effector TH17 and regulatory T cells. Nature. 2006; 441(7090):235–8. [PubMed: 16648838]
63. Colombatti M, et al. Human MBP-specific T cells regulate IL-6 gene expression in astrocytes through cell-cell contacts and soluble factors. Glia. 2001; 35(3):224–33. [PubMed: 11494413]
64. Ogura H, et al. Interleukin-17 promotes autoimmunity by triggering a positive-feedback loop via interleukin-6 induction. Immunity. 2008; 29(4):628–36. [PubMed: 18848474]
65. Ma X, et al. IL-17 enhancement of the IL-6 signaling cascade in astrocytes. J Immunol. 2010; 184(9):4898–906. [PubMed: 20351184]
66. Chauhan D, et al. Identification of upstream signals regulating interleukin-6 gene expression during in vitro treatment of human B cells with pokeweed mitogen. Blood. 1994; 84(7):2243–52. [PubMed: 7919342]
67. D'Aversa TG, et al. Myelin basic protein induces inflammatory mediators from primary human endothelial cells and blood-brain barrier disruption: implications for the pathogenesis of multiple sclerosis. Neuropathol Appl Neurobiol. 2013; 39(3):270–83. [PubMed: 22524708]
68. Sun X, et al. Myelin activates FAK/Akt/NF-kappaB pathways and provokes CR3-dependent inflammatory response in murine system. PLoS One. 2010; 5(2):e9380. [PubMed: 20186338]
69. Stapulionis R, et al. Structural insight into the function of myelin basic protein as a ligand for integrin alpha M beta 2. J Immunol. 2008; 180(6):3946–56. [PubMed: 18322203]
70. Brazda V, et al. Dynamic response to peripheral nerve injury detected by in situ hybridization of IL-6 and its receptor mRNAs in the dorsal root ganglia is not strictly correlated with signs of neuropathic pain. Mol Pain. 2013; 9:42. [PubMed: 23953943]
71. Murphy PG, et al. Endogenous interleukin-6 contributes to hypersensitivity to cutaneous stimuli and changes in neuropeptides associated with chronic nerve constriction in mice. Eur J Neurosci. 1999; 11(7):2243–53. [PubMed: 10383613]
72. Xu XJ, et al. Nociceptive responses in interleukin-6-deficient mice to peripheral inflammation and peripheral nerve section. Cytokine. 1997; 9(12):1028–33. [PubMed: 9417815]
73. Thier M, et al. Interleukin-6 (IL-6) and its soluble receptor support survival of sensory neurons. J Neurosci Res. 1999; 55(4):411–22. [PubMed: 10723052]
74. Bolin LM, et al. Interleukin-6 production by Schwann cells and induction in sciatic nerve injury. J Neurochem. 1995; 64(2):850–8. [PubMed: 7830079]
75. Whitehead KJ, et al. Dynamic regulation of spinal pro-inflammatory cytokine release in the rat in vivo following peripheral nerve injury. Brain Behav Immun. 2010; 24(4):569–76. [PubMed: 20035858]

76. Dublin P, Hanani M. Satellite glial cells in sensory ganglia: their possible contribution to inflammatory pain. Brain Behav Immun. 2007; 21(5):592–8. [PubMed: 17222529]
77. Ledda M, et al. Augmentation in gap junction-mediated cell coupling in dorsal root ganglia following sciatic nerve neuritis in the mouse. Neuroscience. 2009; 164(4):1538–45. [PubMed: 19778588]
78. Huang PP, et al. Spinal botulinum neurotoxin B: effects on afferent transmitter release and nociceptive processing. PLoS One. 2011; 6(4):e19126. [PubMed: 21559464]
79. Zhang J, et al. Myelin basic protein induces neuron-specific toxicity by directly damaging the neuronal plasma membrane. PLoS One. 2014; 9(9):e108646. [PubMed: 25255088]
80. Gahwiler BH, Honegger CG. Myelin basic protein depolarizes neuronal membranes. Neurosci Lett. 1979; 11(3):317–21. [PubMed: 92776]
81. Takasusuki T, Yaksh TL. Regulation of spinal substance p release by intrathecal calcium channel blockade. Anesthesiology. 2011; 115(1):153–64. [PubMed: 21577088]
82. Paez PM, et al. Increased expression of golli myelin basic proteins enhances calcium influx into oligodendroglial cells. J Neurosci. 2007; 27(46):12690–9. [PubMed: 18003849]
83. Smith GS, et al. Classical 18.5-and 21.5-kDa isoforms of myelin basic protein inhibit calcium influx into oligodendroglial cells, in contrast to golli isoforms. J Neurosci Res. 2011; 89(4):467–80. [PubMed: 21312222]
84. Sallmann S, et al. Induction of interleukin-6 by depolarization of neurons. J Neurosci. 2000; 20(23):8637–42. [PubMed: 11102468]

Highlights

- MBP84-104 peptide, injected into an intact nerve, produces long-lasting pain
- IL-6 is the top-induced cytokine by MBP84-104, regardless of T cell content
- Blockade of spinal IL-6 activity reduces MBP84-104-induced pain
- Gabapentin, but not ketorolac, lidocaine or MK801 reverses MBP84-104-induced pain

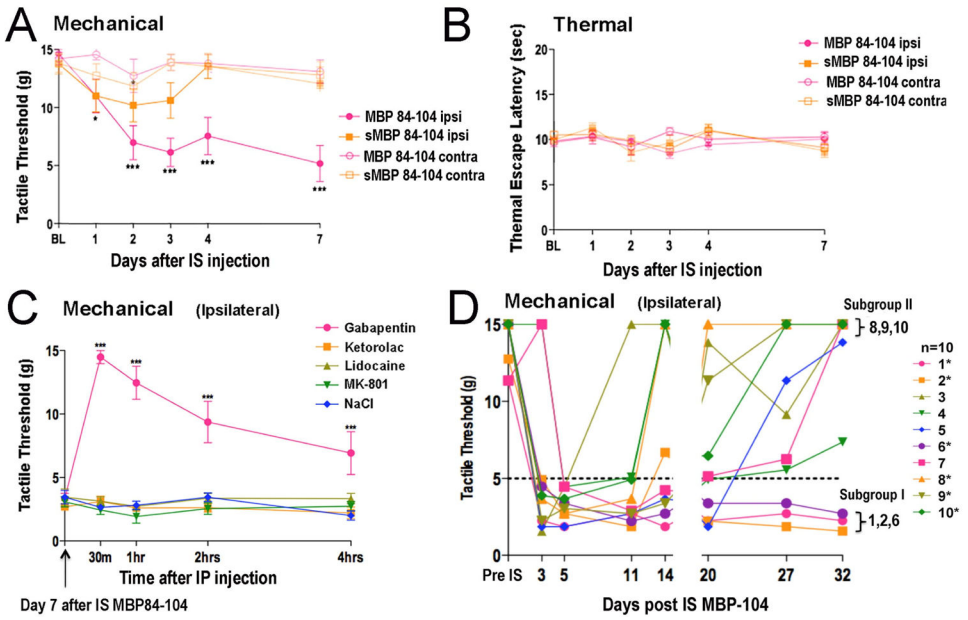

Figure 1. Sustained, unilateral mechanical allodynia induced by MBP is reversed by gabapentin

A, von Frey testing after IS injection of MBP84-104 or scrambled (s)MBP84-104 (50 μg in 5 μl, each, n=10/group) into naïve sciatic nerve. The mean withdrawal thresholds (gram force, g) ± SEM. Within 1 day a decline in mechanical withdrawal thresholds was observed in the ipsilateral hind paw after MBP84-104 but not sMBP84-104 injection. The contralateral hind paws displayed no mechanical hypersensitivity after injection of either peptide**. B,** Hargreaves testing after IS MBP84-104 or sMBP84-104 injection into naïve sciatic nerve (the same animal cohort as in A.). The mean withdrawal latency to thermal stimulation (radiant heat, seconds, s) ± SEM was not changed after injection of either peptide. **C,** The MBP84-104-induced allodynia was reversed by gabapentin (200mg/kg, n=7), but not MK801 (0.05 mg/kg, n=4), ketolorac (30 mg/kg, n=7), lidocaine (2 mg/kg; n=7) or 0.9% NaCl (2 mL/kg, n=6), each administered by IP injection at day 7 after IS MBP84-104. The effect of gabapentin lasted for up to 4 h. ($p \leq 0.05$, ***, $p \leq 0.001$, by 2-way ANOVA with Bonferoni posthoc, comparing to baseline). **D,** Sustained allodynia assessed by von Frey testing for 32 days after IS MBP84-104. Individual withdrawal thresholds in the ipsilateral hind paw (n=10). In all animals, robust allodynia ensued within 3 days and sustained for 11 days post-injection. The subgroup I (n=3, corresponding to 30% of subjects) remained severely allodynic for all 32 days of testing. The subgroup II started to recover at day 13 and reverted to baseline sensitivity by day 32 post-injection.

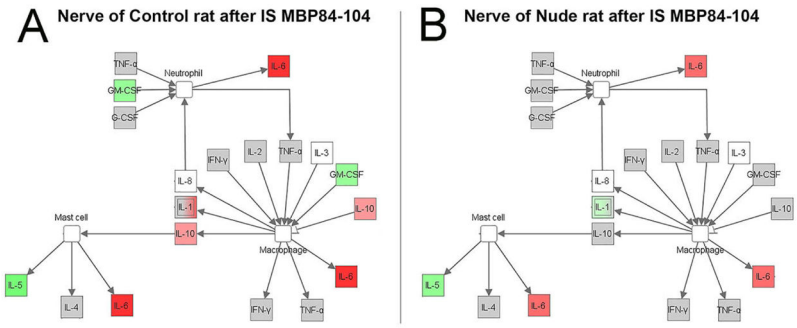

Figure 2. MBP induces IL-6 expression, independent of T cells

Ingenuity Pathway Analysis of Cytokine Gene Network at day 7 after IS injection of MBP84-104 (50 μg in 5 μl, n=6/group) into naïve sciatic nerve of control (**A**) or athymic nude (**B**) rats (right-tailed Fisher's exact test). Upregulated expression of selected cytokine genes in MBP84-104-injected nerves is indicated in red. The intensity of red color corresponds to fold-change of expression levels of respective genes. IL-6 is induced by MBP84-104 injection in both control and athymic nude rats.

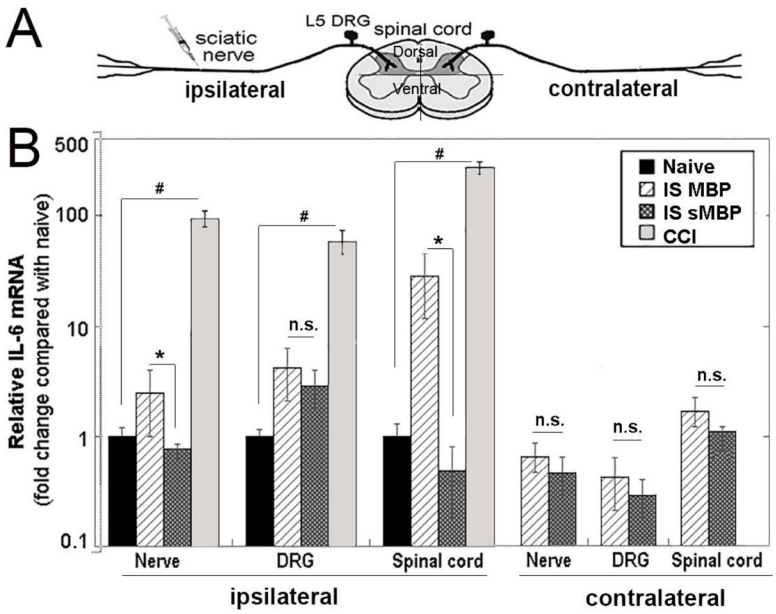

Figure 3. Unilateral increase in spinal IL-6 expression after IS MBP

A, A schematic diagram: after IS injection of MBP84-104 or scrambled (s)MBP84-104 peptides (50 μg in 5 μl, each) into naïve sciatic nerve, ipsilateral or contralateral nerve, DRG and spinal cord (dorsal quarter) samples were analyzed. **B**, IL-6 Taqman qRT-PCR at day 7 after A. or CCI (positive control). The mean relative mRNA ± SEM of n=3–5/group normalized to GAPDH and calibrated to naïve tissues; y, log scale (*, $p \leq 0.05$, n.s., not significant ($p > 0.05$), compared with the scrambled peptide; #, $p \leq 0.05$ compared with naïve; by 2-way ANOVA with Tukey-Kramer posthoc).

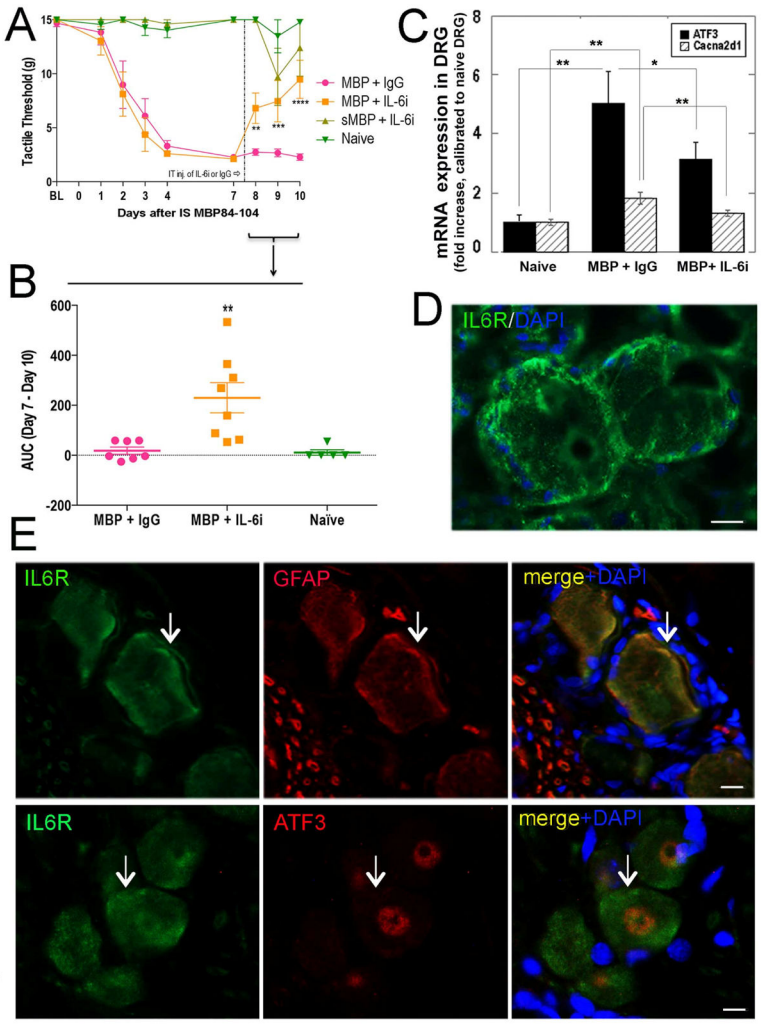

Figure 4. IL-6 inhibitor, intrathecally delivered, reduces MBP-induced allodynia

A, von Frey testing after IS injection of MBP84-104 (n=15) or scrambled (s)MBP84-104 (n=3), 50 μg in 5 μl each, into naïve sciatic nerve, or in naïve rats (n=5). Goat IL-6 function-blocking antibody (IL6i, n=8) or normal goat IgG (n=7), 5 ng/μl each, was delivered IT at day 7 post-IS injection. The withdrawal thresholds in the ipsilateral hind paw showed gradual reduction of mechanical allodynia. **B,** An area-under-the-curve (AUC) analysis of A. from days 7–10 post-injection. The mean withdrawal thresholds (gram force, g) ± SEM (**, p≤0.01; ***, p≤0.001; ****, p≤0.0001, by 2-way ANOVA with Bonferoni post-hoc, comparing to day 7 baseline and excluding sMBP84-104 +IL6i group due to small group size). **C,** ATF3 and Cacna2d1 Taqman qRT-PCR in DRG after completion of A–B, at day 10 post-injection. The mean relative mRNA ± SEM of n=3/group normalized to GAPDH calibrated to naïve DRG (*, p≤0.05; **, p≤0.01, by 2-way ANOVA with Tukey-Kramer posthoc). **D–E,** IL-6R immunofluorescence alone (D–E, green) and dual-stained with GFAP (E, satellite cell marker, red, top panel) or large ATF3+ neurons (E, red, bottom panel) in DRG at day 7 after IS MBP84-104. DAPI (blue). Arrows: co-distribution. Representative of n=4. Scale bars: 15 μm.

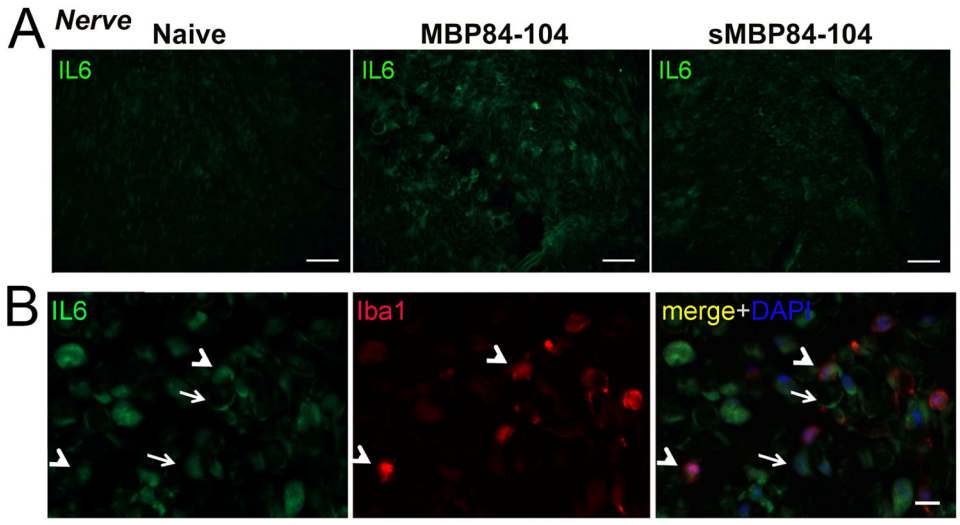

Figure 5. Endoneurial Schwann cells and macrophages express IL-6 after IS MBP

A, IL-6 immunofluorescence (green) in nerve at day 7 after IS injection of MBP84-104 or sMBP84-104 (50 μg in 5 μl, each) into naïve sciatic nerve or in naïve control. **B,** Dual-immunofluorescence of IL-6 (green) with Iba1 (macrophage marker, red) after IS MBP84-104 injection. DAPI (blue). Arrowheads, Iba1+ cells; arrows, crescent-shaped Schwann cells. Representative of n=4/group. Scale bars: A, 40 μm and B, 10 μm.

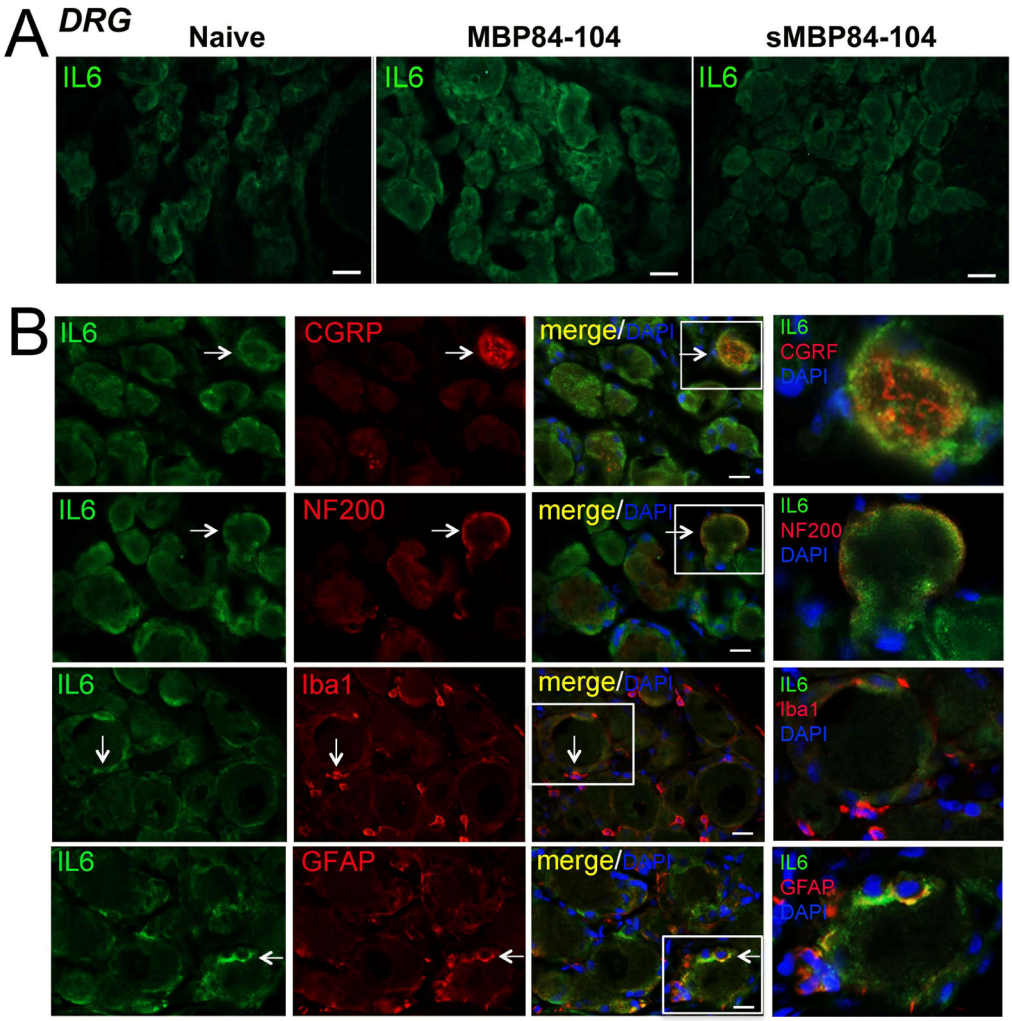

Figure 6. DRG neurons and satellite glia express IL-6 after IS MBP

A, IL-6 immunofluorescence (green) in DRG at day 7 after IS injection of MBP84-104 or sMBP84-104 into naïve sciatic nerve. **B,** Dual-immunofluorescence of IL-6 (green) with NF200 (A-afferent marker, red), CGRP (C-afferent marker, red), GFAP (satellite cell marker, red) or Iba1 (macrophage marker, red) in DRG IS MBP84-104 injection. DAPI (blue). Arrows: co-distribution. Representative of n=4/group. Scale bars: A, 25 μm and B, 10 μm.

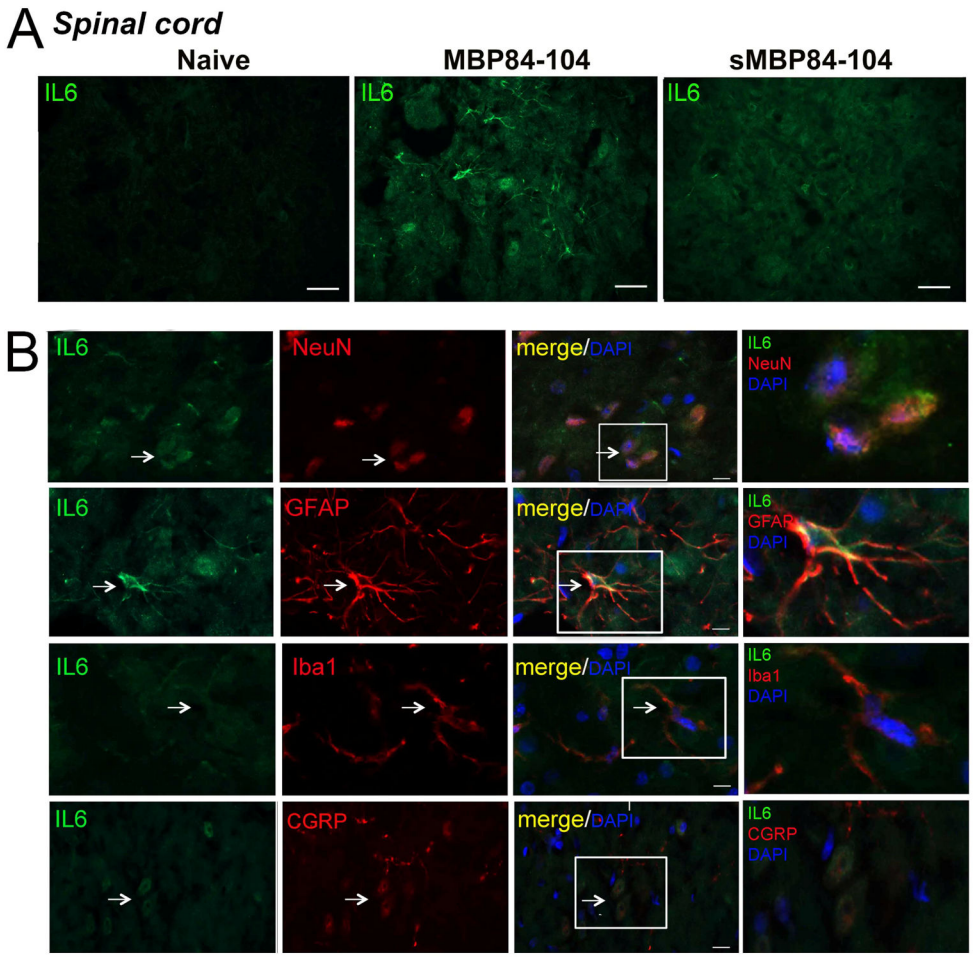

Figure 7. Spinal neurons and astrocytes express IL-6 after IS MBP

A, IL-6 immunofluorescence (green) in ipsilateral dorsal spinal cord at day 7 after IS injection of MBP84-104 or sMBP84-104 into naïve sciatic nerve. **B,** Dual-immunofluorescence of IL-6 (green) with NeuN (neuronal marker, red), CGRP (C-afferent marker, red), GFAP (astrocyte marker, red) and Iba1 (microglia marker, red) after IS MBP84-104 injection. DAPI (blue). Arrows: co-distribution. Representative of n=4/group. Scale bars: A, 25 μm and B, 10 μm.

2.5a Table 1

Primer and probe sequences for *Taqman* qPCR*

Taqman probes contained the 5′-reporter FAM and the 3′-quencher MGB, BHQ-1 or DABCYL dyes. Primers and probes were obtained from Biosearch Technologies, unless indicated otherwise.

Gene	GeneBank #	Sequences (5′-3′)	
ATF3 rat	NM_012912	Forward	TGTCAGTCACCAAGTCTGAGGT
		Reverse	CACTTGGCAGCAGCAATTT
		Probe	Roche #70 (04688937001)
Cacna2d1 rat	NM_012919	Forward	CATACTCCAGATTGGCTGGTG
		Reverse	AGTAGCTGCTGGAGAATAGACCA
		Probe	Roche #74 (0468897001)
GAPDH rat	X02231	Forward	GAACATCATCCCTGCATCCA
		Reverse	CCAGTGAGCTTCCCGTTCA
		Probe	CTTGCCCACAGCCTTGGCAGC
IL-6 rat	NM_012589	Forward	CCCTTCAGGAACAGCTATGAA
		Reverse	ACAACATCAGTCCCAAGAAGG
		Probe	Roche #20 (04686934001)